JOURNAL OF GEOPHYSICAL RESEARCH, VOL. 102, NO. D7, PAGES 8719-8730, APRIL 20, 1997

Measurements of spectral solar UV irradiance in tropical Australia

G. Bernhard, B. Mayer, and G. Seckmeyer

Fraunhofer Institute for Atmospheric Environmental Research, Garmisch-Partenkirchen, Germany

A. Moise

Department of Physics, James Cook University of North Queensland, Townsville, Australia

Abstract. Measurements of global spectral irradiance in the UV and visible range were carried out during December 1995 and January 1996 in Townsville, Australia (19.33°S, 146.76°E, 30 m above sea level (asl)) using the mobile spectroradiometer of the Fraunhofer Institute for Atmospheric Environmental Research, Germany. These are, to our knowledge, the first reported spectral UV measurements in the tropics of Australia. For cloudless days, the spectral measurements are consistent with results of a radiative transfer model. In the UVA, measurement and model agree within ±10% for solar elevations above 10°. In the UVB, the differences are larger (≈15% at 300 nm), which can be explained by uncertainties in the model input parameters of total ozone column and ozone absorption cross section. The variation of the daily erythemal irradiation was found to be ±24% (± 1 σ) for the period of the campaign. The variation of the total ozone column contributes less than ±3% to this variability; the main part is introduced by clouds. These attenuate UV irradiation less than total irradiation (300 nm - 3000 nm); the daily total irradiation averaged over the period of the campaign was reduced by a factor of 0.71 owing to cloudiness compared to the clear-sky case while the erythemal irradiation was only diminished by a factor of 0.78. Using long-term records of total irradiation and ozone column, the parameters influencing UV radiation on Earth were found to be typical for the period and site of the campaign. The maximum erythemally weighted irradiance measured during the campaign was 429 mW/m^2, and the average daily erythemal irradiation for this period was 6.06 kJ/m^2. These high radiation levels were found to exceed the corresponding values for Garmisch-Partenkirchen (47.5°N, 11.0°E, 730 m asl), Germany, by between 55 and 70%. This pronounced difference in the radiation environment between Australia and Germany is explained by the higher solar elevation and the lower ozone column in the tropics.

1. Introduction

In the tropics, high levels of solar UV radiation are present throughout the whole year because of high solar elevations and relatively low total ozone columns compared to midlatitudes. There is evidence that high levels of ambient UV radiation affect public health detrimentally as follows: epidemiological studies revealed a correlation between the increase of skin cancer incidence and UV exposure in white populations; Caucasians living in regions near the equator have the highest risk of getting skin cancer [*Schaart et al.*, 1993]. An Australia wide survey in 1990 estimated an age-standardized incidence rate for nonmelanoma skin cancer (NMSC) of 977 per 100,000 inhabitants, which documents an increase of 19% compared with results found by an earlier study in 1985 [*Marks et al.*, 1993]. A strong latitudinal gradient of the incidence rates was found; NMSC rates in latitudes less than 29°S are over 4 times the rates in latitudes greater than 37°S. For a community in Queensland, Australia, incidence values for NMSC were reported to be as high as 2389/100,000 (males) and 1908/100,000 (females) [*Schaart et al.*, 1993; *Green and Battistutta*, 1990]. The increasing number of people traveling from midlatitudes to tropical regions for recreation further supports the importance of the determination of UV levels in this part of the world.

Besides the situation in the tropics, the worldwide observed decline of stratospheric ozone [*Bojkov*, 1995] has raised concern about increasing solar UV radiation at the Earth's surface [*McKenzie et al.*, 1994]. A worldwide change of the radiation environment could have serious consequences on the biosphere including mankind and terrestrial and aquatic ecosystems [*Caldwell and*

Paper number 97JD00072.
0148-0227/97/97JD-00072$09.00

Flint, 1994]. Up until now, there has been almost no ozone trend in the tropics, but owing to the high ambient UV levels and low ozone columns, the situation at this location can be considered as a "worst case scenario" for midlatitudes if total ozone columns would decrease dramatically in future decades. Therefore the presented measurements and evaluations may be relevant for a large community investigating UV effects in Australia and in other parts of the world.

The measurement of solar UV radiation became only recently a topic of growing interest, and therefore only few systematic measurements were performed before the 1990s. In Australia, D. F. Robertson started to investigate the relation between solar ultraviolet radiation, sunburn, and skin cancer in the 1960s [*Robertson*, 1972]. He developed a broadband sensor with a spectral sensitivity similar to the action spectrum of erythema [*McKinlay and Diffey*, 1987]. This device is well known as the "Robertson Berger meter" (RBM). The latest versions of RBM-type sensors are now used at many locations worldwide. During extensive investigations between 1963 and 1970, Robertson monitored the erythemally weighted irradiance at five locations in Australia and New Guinea between 6.1°S (Goroka, New Guinea) and 38°S (Melbourne, Australia) with his sensors. Since these measurements are related to the instrument-based "sunburn unit", it is difficult to transform Robertson's results to physical units that would allow a comparison with current measurements.

Between 1975 and 1981, the Australian Commonwealth Scientific and Industrial Research Organization (CSIRO) operated a network of detectors with a similar design as Robertson's instrument [*Barton*, 1983]. According to this report, the sensors were not suited to detect a small long-term trend in the UVB irradiance due to a change in total atmospheric ozone content because of drifts of the sensors' sensitivity; but the instruments of the CSIRO network were found to provide sufficient data for a geographic and seasonal climatology of UVB over Australia.

The Australian Radiation Laboratory (ARL) has been involved for many years in the measurement of solar UV radiation using spectroradiometers, and a network of broadband detectors at 20 sites in Australia and Antarctica was established in the early 1980s [*Gies et al.*, 1994; *Roy et al.*, 1995]. Apart from other sensors, most stations are now equipped with model 501 UV biometers. The broadband detectors are regularly intercompared, and further quality control is performed by the comparison of broadband with spectroradiometric measurements. The ARL spectroradiometer successfully took part in international intercomparison campaigns [*McKenzie et al.*, 1993; *Seckmeyer et al.*, 1995].

Up until now, all continuous measurements of solar UV radiation in tropical Australia were carried out with broadband sensors. Here we present the first reported measurements of spectrally resolved solar UV irradiance in the tropics of Australia. Spectral measurements are considered to be more reliable than measurements carried out with broadband instruments since the calibration of spectroradiometers can be related more accurately to primary standard radiation sources. A second advantage of spectral measurements is that they contain much more information than broadband measurements: (1) solar spectra can be weighted with any action spectra, i.e., in order to address different biological effects, (2) spectral data are more suitable to evaluate radiative transfer models, and (3) spectral data allow the extraction of information about the atmospheric condition during the measurement (e.g., total ozone column), which allows the study of the processes and parameters that influence UV radiation on Earth.

The realization of this study was further encouraged by the fact that ground-based spectral UV measurements are generally very sparse at other tropical locations of the world. An example of a more recent activity is the installation of a spectroradiometric system on Mauna Loa, Hawaii, in 1994 within the Network for the Detection of Stratospheric Change (NDSC) by New Zealand's National Institute of Water and Atmospheric Research (NIWA) and the National Oceanic and Atmospheric Administration (NOAA), Boulder, Colorado [*Bodhaine et al.*, 1996].

2. Site, Period, Instrument and Methodologies

2.1. Site and Period of the Spectral Measurements

All spectral measurements were performed with the mobile spectroradiometer of the Fraunhofer Insitute for Atmopheric Environmental Research (IFU). On December 21, 1995, this instrument was set up near Townsville, Australia, on the roof of the Physics Department of the James Cook University (JCU) of North Queensland (19.33°S, 146.76°E, 30 m above sea level (asl)). In the northern direction, the horizon was slightly hidden by parts of the building. In the southeastern direction, the horizon was limited by Mount Stuart (2.7 km remote, 560 m asl). Owing to the restriction of the horizon, the diffuse radiation at the place of the spectroradiometer is reduced by approximately 1.5%. The surface condition of the surroundings in the west, south, and east is characterized by clear forests and grassland; in the northern direction, there are the houses and gardens of Townsville.

Measurements of solar spectral irradiance were carried out between December 24, 1995, and January 20, 1996. At the beginning of the campaign, the solar elevation at noon was 86° and at the end, 89°. Most days were partly cloudy, but January 11 was nearly a clear-sky day. Between January 5 and 8, heavy storms and rainfall occurred.

2.2. Mobile IFU Spectroradiometer

The mobile IFU spectroradiometer consists of a horizontal cosine-response diffuser coupled by quartz fiber optics to a double monochromator DTM 300 from Bentham instruments (focal length, 300 mm; focal ratio,

$f/4.1$). For the wavelength range 285 nm - 500 nm, holographic gratings with 2400 lines per millimeter are used and radiation leaving the monochromator is chopped, detected with a bialkali-photomultiplier (9205QB, EMI) and amplified using lock-in technique. For this wavelength range, the nominal bandwidth of the monochromator is 0.5 nm full width at half maximum (FWHM) and the measured bandwidth is 0.58 nm FWHM. For wavelengths above 500 nm ruled gratings with 600 lines per millimeter are applied, the nominal bandwidth is 2 nm FWHM (measured 2.3 nm FWHM), and the radiation is detected with a Si-diode. Below 410 nm, measurements were taken in 0.25 nm increments and above 410 nm, in 1 nm steps. During the campaign, the whole system was maintained at 33 ± 0.5°C and was fully controlled by a PC. Since solar elevation and atmospheric conditions are changing during a scan, the exact time was stored together with each data point.

Two different entrance optics of the spectroradiometer were tested during the campaign. Between January 4 and 11, measurements were carried out using a diffuser which underestimates incident isotropic radiation by a factor of 0.93, and for the rest of the campaign newly developed entrance optics were used which measure isotropic radiation correctly within 3% and thus meet the specification of the NDSC (R. L. McKenzie et al., UV spectro-radiometry in the network for the detection of stratospheric change, submitted to *NATO ASI Series*, 1996). Appropriate corrections for the deviation of the angular response of both entrance optics from the ideal cosine response were applied; details of this algorithm are given by *Seckmeyer and Bernhard* [1993]. After this correction, remaining uncertainties due to deviations from the ideal cosine response contribute less than 4% to the overall error budget. For more details about the spectoradiometer, see *Seckmeyer et al.* [1996]. The spectral measurements were supplemented by measurements of a luxmeter (Tageslichtmeßkopf 910G from PRC Krochmann, Berlin) and a pyranometer (model CM11, Kipp&Zonen).

2.3. Calibration of the Spectroradiometer

The calibration of the absolute sensitivity was carried out on the roof of JCU using 100 W tungsten halogen lamps and a transportable lamp housing which avoids transportation of the spectroradiometer between calibration and solar measurement. The calibration was checked seven times during the campaign and was found to be stable within ±2%; corrections for these small drifts of the instrument's sensitivity were applied. The calibration of the 100 W lamps refers to a transfer standard (1000 W tungsten halogen lamp type FEL), which was itself calibrated by the Physikalische Technische Bundesanstalt (PTB), Germany. According to PTB, the uncertainty of the transfer standard's calibration is ±3% (±2 σ) for wavelengths between 270 and 400 nm and ±1.6% in the range 400 – 800 nm.

The wavelength calibration of the spectroradiometer was carried out by means of a low-pressure mercury lamp and was checked for wavelengths in between the mercury lines by comparison of the measured spectra with an extraterrestrial spectrum which was measured by the solar ultraviolet spectral irradiance monitor (SUSIM) during the ATLAS 2 mission in 1993 [*Woods et al.*, 1996]. For the whole campaign, the accuracy of the alignment was found to be within ±0.06 nm in the UV range.

2.4. Quality Control and Quality Assurance

Besides careful wavelength alignment and absolute calibration, the spectral measurements in the visible range were weighted with the sensitivity function of the human eye [*German Institute of Standardization*, 1982] and compared with concurrent measurements of the luxmeter. The weighted and cosine-corrected spectral measurements agreed with the luxmeter readings within ±5% for solar elevations above 20°.

The IFU mobile spectroradiometer showed its reliability in two intercomparison campaigns of UV spectroradiometers, one held in Garmisch-Partenkirchen, Germany, in August 1994 [*Seckmeyer et al.*, 1995] and one held in Ispra, Italy, in May 1995; from the measurements of global spectral irradiance sampled during the Garmisch-Partenkirchen campaign, the daily, erythemally weighted irradiation was calculated. The values found by the groups participating in this campaign agreed within ±7%. The same methodologies were applied for the austral campaign and these intercomparison campaigns.

2.5. Ozone Column Derived From Spectral Measurements

Model calculations of UV irradiance require total ozone column and the aerosol optical depth. These parameters were determined from the spectral measurements; alternately, with the measurements of global spectral irradiance, seven scans of diffuse irradiance were carried out on January 11 by shading the disk of the Sun. Subtracting diffuse from global measurements, spectra of direct irradiance were calculated. From the direct spectra, the total ozone column and the aerosol optical depth were calculated. Ozone columns determined with this method from measurements of direct irradiance at IFU in Garmisch-Partenkirchen have been compared earlier with Brewer values from the Meteorological Observatory Hohenpeißenberg, which is about 50 km from IFU [*Jäger et al.*, 1996]. The systematic deviation of the values derived at both sites was only 1%, and the standard deviation was ±1.5%.

For January 11, the ozone column derived from the global/diffuse measurements in Townsville was 262 Dobson units (DU). This value was used as input for model calculations and was compared with TIROS operational vertical sounder (TOVS) satellite data supplied by the Bureau of Meteorology, Melbourne, Australia. The TOVS measurement was 250 DU, which is 4.8% less than the IFU measurement. However, according to *Harris* [1994], TOVS data show significant variance (that is, $\approx$ ±3% difference between TOVS and total ozone mapping spectrometer (TOMS) satellite data

is reported for monthly averages of zonal (30°- 50°N) means for the years 1979 to 1993), and therefore parts of the deviation of 4.8% can be explained by uncertainties of the satellite measurements.

The optical depth for aerosol scattering and absorption was determined to be below 0.1 at 340 nm. This is consistent with earlier observations [*Seckmeyer and McKenzie*, 1992] which suggest that the aerosol loading of the atmosphere is generally less pronounced in the southern hemisphere compared with the northern hemisphere.

In order to obtain ozone values for cloudy days, where no determination of the direct irradiance is possible, a method was applied which uses the measurements of global irradiance as suggested by *Stamnes et al.* [1991]. According to this method, the global irradiance at 305 nm (strong ozone absorption) and 340 nm (weak ozone absorption) is compared with model results at the same wavelengths. For noon of January 11, the ozone column was calculated to be 257 DU, which is 5 DU (or 2%) less than the value obtained by the "direct" method. For the analysis of the day-to-day variability of solar UV radiation during the campaign, ozone values were used which were calculated according to this "global" method; the average ozone column for the period of the campaign was found to be 257 ±6 DU (±1 σ). Thus the day-to-day variation in ozone column was ±2.3%.

2.6. Calculation of Biologically Effective Radiation

In order to assess biological effects of UV radiation, the measured spectra of global irradiance $E(\lambda)$ in units of mW/(m^2 nm) were weighted with the Commission Internationale de l'Éclairage (CIE) action spectrum for erythema (sunburn) [*McKinlay and Diffey*, 1987] and with the action spectrum of DNA damage [*Setlow*, 1974]:

$$E_{\text{bio}} = \int_{285\text{ nm}}^{400\text{ nm}} E(\lambda) \cdot A(\lambda)\, d\lambda \qquad (1)$$

where $A(\lambda)$ is the action spectrum of the corresponding effect and E_{bio} is the weighted result.

Until recently, there was no accepted formula for the parameterization of the DNA action spectrum given by *Setlow* [1974], and therefore it is quite difficult to compare values of DNA weighted irradiance measured by different groups. To overcome these difficulties, the following parameterization was proposed by the NDSC steering committee and will be used in this paper to calculate DNA damaging radiation:

$$A_{\text{DNA}}(\lambda) := \begin{cases} \frac{1}{0.0326} \cdot \exp\left[13.82 \cdot \left(\frac{1}{1+\exp[(\lambda\,[\text{nm}]-310)/9]}-1\right)\right], & \lambda \le 370\text{ nm} \\ 0, & \lambda > 370\text{ nm} \end{cases} \qquad (2)$$

According to (1), the erythemally weighted irradiance E_{bio} has the physical unit milliwatts per square meter, and this unit will be used throughout this paper. However, for public information, the unit "med" is often used. Depending on the definition [*World Health Organization*, 1994], one med corresponds to 200-300 J/m^2 of erythemally weighted irradiation on a horizontal surface; a common definition is 1 med = 210 J/m^2. According to this relation, one med per hour (med/h) corresponds to 58.3 mW/m^2 of erythemally weighted irradiance; e.g. the maximum erythemally weighted irradiance measured during this campaign of 429 mW/m^2 (see section 4) corresponds to 7.4 med/h, which is equivalent to 8 min to receive 1 med.

Alternatively to med, the "UV index" was proposed recently [*International Commission on Non-Ionizing Radiation Protection*, 1995]. The UV index is defined as daily maximum erythemally weighted irradiance in Watts per square meter, averaged over a duration of between 10 and 30 minutes and multiplied by 40. Assuming that the radiation conditions remained constant during 10 minutes, the highest value of erythemally weighted irradiance measured during the campaign of 429 mW/m^2 corresponds to an UV index of 17.

3. Results for Clear-Sky Conditions

3.1. Global Spectral Irradiance

Corresponding to the duration of a scan, approximately every 13 min, a spectrum of global spectral irradiance was measured between 285 and 1100 nm (650 nm after January 4). Figure 1 shows a spectrum that was measured at noon on January 11, 1996, a day with nearly cloudless sky; the global spectral irradiance in the UVB (280 - 315 nm) and UVA (315 - 400 nm) is plotted on a linear and logarithmic scale. The solar zenith angle (SZA) during the scan was approximately 3°. The sharp increase of the spectrum over several orders of magnitude in the UVB range is caused by the absorption in the ozone layer. In the UVA, the

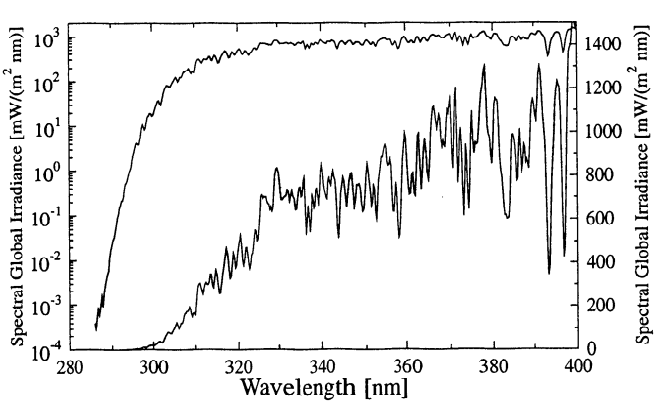

Figure 1. Spectral global irradiance, January 11, 1996, 3° solar zenith angle (SZA) on a linear (right axis) and logarithmic (left axis) scale. The sharp increase of the spectrum over several orders of magnitude in the UVB range is caused by the absorption due to atmospheric ozone, and the fluctuation in the UVA is due to the Fraunhofer structure in the solar spectrum.

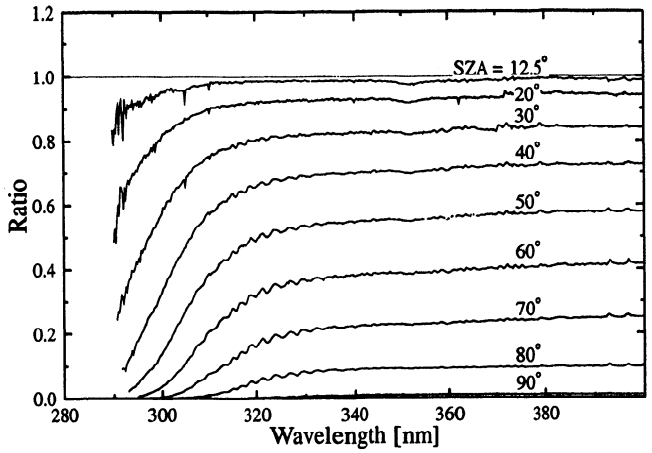

Figure 2. Ratios of spectra of global irradiance at different SZAs to the spectrum at 5° SZA. The spectra at definite SZAs are interpolated using the data which were recorded on January 11. Below 340 nm, the wavy structure in the ratios is caused by the ozone cross section. With larger SZA, the short wave end of the solar spectrum is shifted toward longer wavelengths. The remaining structure in the ratios is attributable to small clouds (that is, the small dip at 352 nm is caused by clouds during noon which affect the interpolated spectrum at 5° SZA).

Fraunhofer structure of the solar spectrum can clearly be seen. The detection limit (ratio signal/noise = 2) is 1 μW/(m^2 nm). For the presented spectrum, the detection limit is reached at 288 nm.

In order to obtain spectra of global irradiance for definite SZAs, the spectra measured on January 11, 1996, were interpolated to SZAs in increments of 2.5° using natural cubic splines. Figure 2 illustrates the dependence of these spectra on SZA and shows the ratio of spectra at different SZA to the spectrum at 5° SZA for the irradiance higher than 10 μW/(m^2 nm). Between 340 and 400 nm, the change of global irradiance with SZA depends only slightly on wavelength. Below 340 nm, the ozone absorption becomes apparent; especially for SZAs above 60°, the wavy structure in the ozone cross section can clearly be seen.

The spectra at fixed SZAs used for Figure 2 are listed in Table 1. To reduce the data set for presentation (744 data points per spectrum), the spectra were convoluted with triangular functions of bandwidth 1 nm FWHM (300 - 310 nm), 2 nm FWHM (310 - 340 nm), 5 nm FWHM (340 - 400 nm), and 10 nm FWHM (400 - 650 nm). Below 300 nm, the data were not convoluted.

3.2. Comparison of Measured Spectra With Model Results

The spectra measured on January 11 were compared with results from the radiative transfer model UVSPEC, type pseudospherical, developed by A. Kylling (available by ftp kaja.gi.alaska.edu, cd /pub/arve) [*Stamnes et al.*, 1988]. The model was adapted to the data format of the measurements in order to provide one model value for each measured data point. The model values at each wavelength refer to the actual measurement time at this wavelength. The model input parameters are extraterrestrial spectrum (convoluted with the slit function of the spectroradiometer), SUSIM/ATLAS 2 [*Woods et al.*, 1996]; ozone, pressure, and temperature pro-

Table 1. Global Spectral Irradiance Measured on January 11, 1996, for Different Solar Zenith Angles

Wavelength,	Global Spectral Irradiance, mW/(m^2 nm)							
nm	70°	60°	50°	40°	30°	20°	12.5°	5°
290	...	...	...	...	...	0.0112	0.0181	0.023
290.5	...	...	...	...	...	0.017	0.0291	0.0352
291	...	...	...	...	0.0146	0.0328	0.0496	0.0545
291.5	...	...	...	...	0.0308	0.07	0.0974	0.1064
292	...	...	...	0.016	0.0537	0.1097	0.1477	0.1711
292.5	...	...	...	0.0182	0.0682	0.138	0.1982	0.2132
293	...	...	...	0.0458	0.1345	0.2693	0.3561	0.4048
293.5	...	...	0.015	0.0747	0.219	0.3955	0.5351	0.5934
294	...	...	0.0249	0.1164	0.3173	0.5493	0.7274	0.8015
294.5	...	...	0.038	0.1671	0.4345	0.7638	0.9926	1.102
295	...	...	0.0708	0.2947	0.7113	1.190	1.541	1.681
295.5	...	0.0177	0.1291	0.503	1.178	1.961	2.510	2.722
296	...	0.03	0.2292	0.7948	1.803	2.900	3.631	3.940
296.5	...	0.0373	0.2637	0.8393	1.812	2.930	3.582	3.906
297	...	0.0581	0.3724	1.109	2.314	3.592	4.453	4.786
297.5	0.0129	0.1424	0.7902	2.274	4.521	6.845	8.426	9.032
298	0.0154	0.1835	0.8845	2.518	4.888	7.441	8.988	9.551
298.5	0.018	0.2098	0.9678	2.555	4.820	7.151	8.494	9.082
299	0.0428	0.4273	1.815	4.645	8.721	12.74	15.10	16.04
299.5	0.0662	0.6052	2.499	5.999	10.74	15.42	18.03	19.18
300	0.0657	0.6207	2.345	5.515	9.596	13.60	15.94	16.76
301	0.1987	1.447	4.931	10.71	17.70	24.15	27.82	29.10
302	0.3881	2.435	7.505	15.24	24.15	32.10	36.66	38.30

Table 1. (continued)

Wavelength,	Global Spectral Irradiance, mW/(m^2 nm)							
nm	70°	60°	50°	40°	30°	20°	12.5°	5°
303	0.9753	5.463	15.39	29.43	45.00	58.57	65.89	68.95
304	1.544	7.726	20.34	37.20	55.27	71.12	79.22	83.05
305	2.843	12.33	29.85	51.77	74.18	94.76	103.70	109.41
306	3.736	14.94	33.82	57.08	80.34	100.26	110.40	114.85
307	6.334	22.43	47.44	76.91	105.8	130.1	143.0	147.7
308	9.097	29.54	60.36	95.21	128.6	156.7	171.5	177.0
309	10.33	31.08	61.12	94.47	125.6	151.8	165.6	170.4
310	14.46	39.71	73.90	110.7	144.6	172.9	187.5	192.5
312	27.06	67.23	118.6	171.8	220.2	259.7	281.1	286.4
314	36.82	83.97	141.3	199.6	249.6	291.5	314.1	320.0
316	45.82	97.25	157.5	216.0	267.0	309.3	332.3	338.4
318	60.46	121.8	192.5	258.8	316.9	364.9	391.6	397.8
320	75.25	145.6	224.4	298.4	362.8	414.9	444.5	451.3
322	79.35	149.2	226.1	298.1	360.2	410.4	439.1	445.8
324	94.92	173.6	258.5	337.9	405.3	459.8	490.7	498.4
326	128.7	231.7	341.8	444.4	530.9	601.5	641.7	651.0
328	138.2	245.6	360.9	467.6	556.9	630.4	672.3	681.2
330	157.2	275.5	402.8	518.8	616.1	696.7	742.1	752.6
332	150.6	262.6	382.3	491.1	582.5	656.4	699.3	710.2
334	154.2	266.9	388.1	497.8	589.2	664.1	706.2	717.0
336	146.5	251.8	364.4	466.5	550.5	621.2	659.9	669.4
338	151.0	260.0	374.8	478.8	565.3	636.9	677.4	686.7
340	170.1	292.4	420.7	536.4	633.4	711.3	756.1	767.3
345	166.3	284.5	407.4	518.3	609.8	684.5	726.5	738.3
350	181.6	308.9	441.5	560.4	658.5	737.2	781.6	799.3
355	190.2	323.7	462.0	585.9	687.0	770.6	815.8	832.8
360	183.0	311.8	444.6	564.0	661.1	738.1	781.3	794.5
365	221.4	376.2	535.0	677.1	791.3	880.3	932.0	945.9
370	236.3	400.1	567.9	717.5	834.6	931.0	985.0	997.8
375	222.6	375.9	531.4	669.9	782.3	873.1	921.3	929.6
380	234.0	394.4	557.0	701.4	818.9	916.5	963.7	971.1
385	205.5	345.3	485.3	608.7	709.0	794.1	834.9	842.3
390	242.9	406.5	569.5	714.1	830.7	929.1	977.0	986.8
395	235.8	393.0	548.4	686.7	797.6	890.8	936.6	948.8
400	355.9	592.2	823.9	1031	1196	1335	1404	1423
410	408.0	675.5	932.4	1162	1347	1499	1577	1598
420	426.5	702.6	965.6	1202	1389	1545	1623	1646
430	401.0	656.8	900.9	1119	1291	1435	1507	1527
440	472.3	768.5	1052	1305	1504	1668	1753	1775
450	526.2	852.8	1164	1441	1658	1834	1929	1954
460	546.5	880.8	1198	1481	1701	1882	1978	2006
470	545.9	878.6	1192	1470	1688	1865	1966	1992
480	550.7	883.3	1200	1478	1697	1873	1973	1997
490	533.2	850.0	1149	1415	1620	1789	1880	1906
500	534.9	853.2	1151	1417	1622	1791	1883	1910
510	522.8	831.7	1122	1381	1581	1747	1835	1860
520	510.6	809.2	1090	1341	1533	1696	1781	1805
530	528.4	837.9	1131	1392	1592	1762	1850	1878
540	521.6	826.8	1115	1374	1572	1740	1829	1857
550	520.5	825.4	1112	1370	1568	1738	1826	1855
560	507.8	805.1	1087	1339	1535	1702	1791	1819
570	487.4	780.2	1060	1310	1505	1672	1761	1791
580	484.9	776.0	1053	1303	1499	1666	1755	1787
590	453.5	731.4	996.7	1236	1427	1588	1677	1711
600	461.7	738.2	1001	1240	1430	1591	1682	1719
610	465.6	734.8	991.6	1226	1412	1573	1664	1705
620	451.3	711.2	958.4	1186	1369	1528	1618	1663
630	429.7	679.6	918.3	1140	1318	1475	1566	1617
640	427.8	668.7	901.1	1115	1292	1447	1540	1599
650	401.9	631.4	857.1	1062	1235	1384	1479	1546

Bandwidth below 300 nm is 0.58 nm fullwidth at half maximum (FWHM), that at 300 nm – 310 nm is 1 nm FWHM, at 310 nm – 340 nm is 2 nm FWHM, that at 340 nm - 400 nm is 5 nm FWHM, and at 400 nm – 650 nm is 10 nm FWHM.

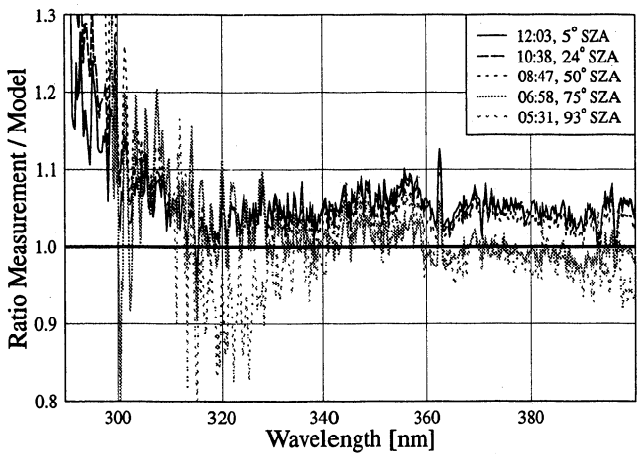

Figure 3. Ratio of measured and modeled global irradiance for January 11 and several SZAs. The time and SZA refer to the values at 350 nm.

files, U.S. standard atmosphere [*Anderson et al.*, 1986]; ground albedo = 0.02; total ozone column = 262 DU; visibility = 200 km; background volcanic aerosol.

Figure 3 shows the ratio of measured and modeled spectra for January 11 at different SZAs. The ratios are displayed for spectral irradiance higher than 10 μW/(m^2 nm), which is 10 times above the detection limit. The ratios depend only slightly on solar elevation; even if the Sun is below the horizon (SZA = 93°), the agreement is remarkably good. In the UVA, the deviation between measurement and model for all wavelengths and solar elevations is smaller than ±10%. Below 315 nm, the ratio becomes very sensitive to the total ozone column and the ozone cross section [*Molina and Molina*, 1986] used in the model. At 300 nm, a -1% change in total ozone column leads to a 3% change in spectral irradiance. At the same wavelength, the uncertainty of the spectroradiometer's wavelength alignment of ±0.06 nm leads to ±3% uncertainty in the spectral irradiance. The increasing deviation of the ratios at shorter wavelength can partly be explained by these uncertainties.

Figure 4 shows the diurnal variation of the ratios of measured and modeled global irradiance in more detail. Both measured and modeled spectra were averaged over 10 nm wavelength bands, and the ratios were plotted as a function of time. At noon, the measurements are about 5% higher than the model results. Generally, between 0700 and 1700 (which corresponds to 74° and 65° SZA), the ratios are close to unity, except at two times around noon when the measurements were disturbed by small clouds. The dependence of the ratios on wavelength is rather small. Only a small part of the ratio's dependence on SZA can be attributed to the remaining uncertainty after the cosine correction. The good agreement between measurements and model results demonstrates that the model is suitable to calculate the UV irradiance for clear sky under tropical atmospheric conditions.

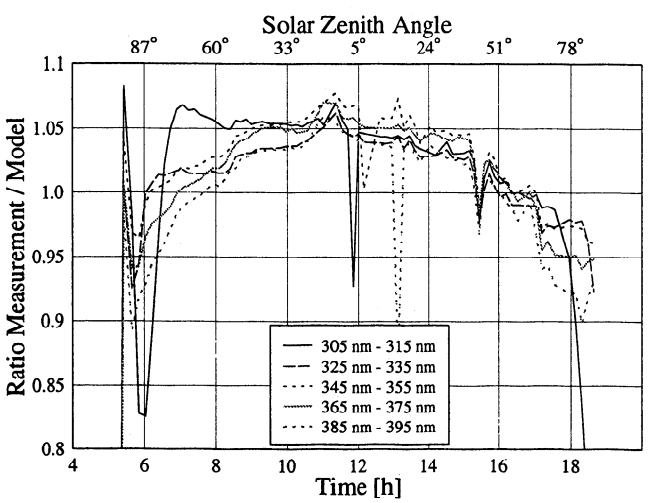

Figure 4. Diurnal variation of ratios of measured and modeled global irradiance for January 11. Both measured and modeled spectra were averaged over 10 nm wavelength bands (see legend) before forming the ratio.

4. Results for All-Sky Conditions

4.1. Diurnal Variations

In most situations, clouds attenuate UV radiation, but when the disk of the Sun is not obscured, additional radiation can be reflected from the edges of the clouds to the radiometer causing an increase of the radiation.

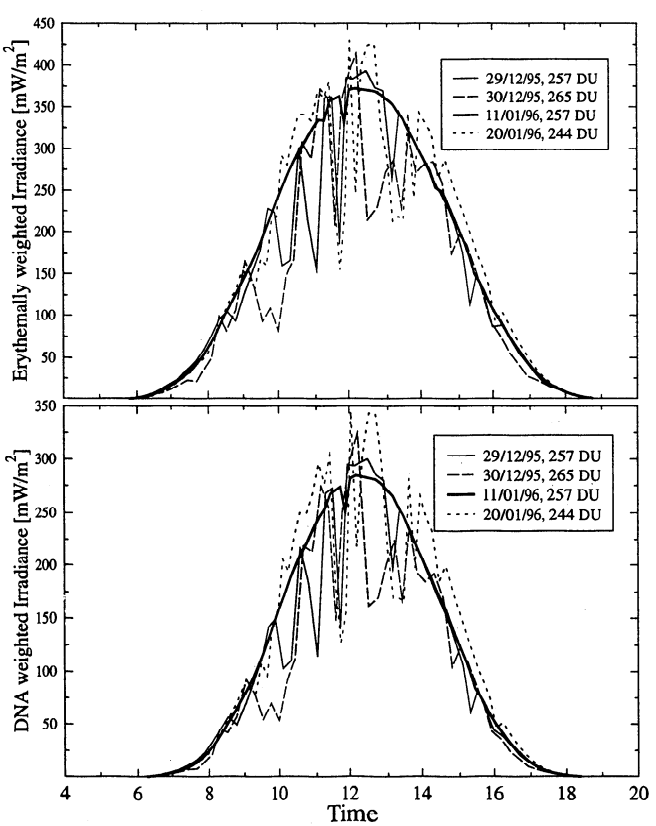

Figure 5. Diurnal variation of (top) erythemally and (bottom) DNA weighted global irradiance.

This was already found in earlier studies [e.g. *Nack and Green*, 1974].

The diurnal variation of the erythemally and DNA weighted global irradiance for various days is shown in Figure 5. The highest values of erythemally and DNA weighted irradiance were measured around noon on January 20, a day with relatively low total ozone column (244 DU) and broken-cloud conditions, the maximum value of erythemally weighted irradiance was 429 mW/m^2, and the maximum value of DNA weighted irradiance was 345 mW/m^2. The highest values measured on the nearly cloud free day of January 11 were 372 mW/m^2 (erythema) and 284 mW/m^2 (DNA), respectively. Ozone column and solar elevation contribute 6% to this 15% difference in erythemally weighted irradiance between January 11 and 20; the major part of the difference is attributable to cloud effects.

4.2. Day-to-Day Variations

For the period of the campaign, the day-to-day variation of the erythemally weighted irradiance is predominantly affected by differences in cloud cover. To illustrate this variability, Figure 6 shows the variation of doses of the erythemally weighted radiation. These were calculated by integrating the erythemally weighted global irradiance over time for the periods 1100 - 1300, 1000 - 1400, 0900 - 1500, and for the whole day. For January 11, the daily erythemally weighted dose was 7794 J/m^2. In addition, the mean value of 6055 J/m^2 and the standard deviation (1462 J/m^2) of the daily doses are plotted. This variability is ±24% (± 1 σ). The daily dose on January 6, a day with heavy thunderstorms, is 20% of the dose on January 11. Figure 6 shows that more than half of the daily dose is cumulated between 1000 and 1400. This is even the case for rather cloudy days.

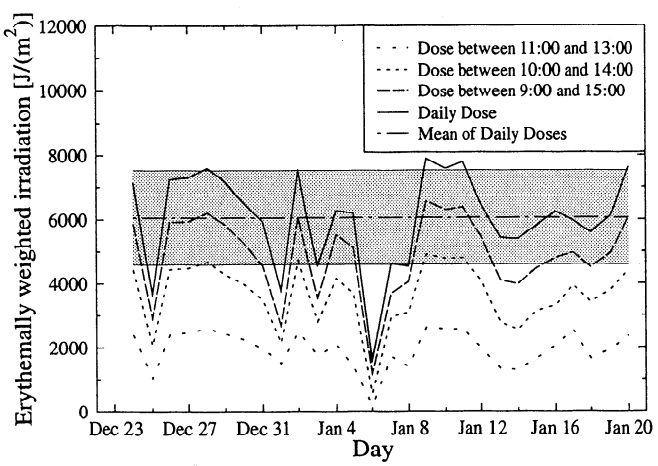

Figure 6. Erythemally weighted irradiation for all days of the campaign and for different periods of the day. The shaded area illustrates the area of ±1 σ around the mean of the daily doses.

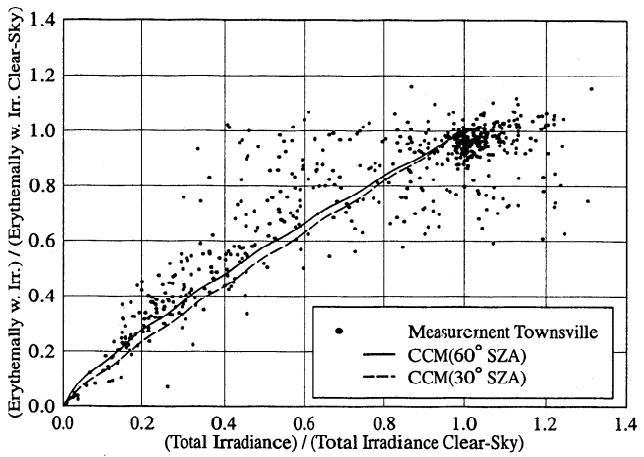

Figure 7. Reduction R_{ery} of erythemally weighted irradiance versus reduction of total irradiance R_{total} due to attenuation by clouds. The dots represent the measurements in Townsville for SZA between 30° and 60°. "Cloud cover modifier" (CCM) functions for SZA = 30° and SZA=60° as suggested by *Bodeker and McKenzie* [1996] are depicted for comparison.

4.3. Erythemally Weighted Irradiance Versus Total Irradiance for Cloudy-Sky Conditions

A quantitative investigation of clouds on erythemally effective radiation is complicated since cloud properties are difficult to parameterize. This will be a challenging task for future work and cannot be addressed in this paper in detail. However, in order to give an estimate of the effect of clouds, the pyranometer data were correlated with the measurements of erythemally weighted irradiance similar to the analyses by *Bordewijk et al.* [1995] and *Bodeker and McKenzie* [1996]. In the following, the change of the erythemally weighted irradiance due to clouds compared to the clear-sky case will be related to the respective change of the total global irradiance (≈ 300 - 3000 nm) measured by the pyranometer.

The clear-sky values were taken from the measurements of January 11. In order to separate the influence of the ozone column from the influence of clouds, the erythemally weighted irradiance of all days was normalized to the ozone column of January 11. For this normalization procedure, it was assumed that a +1% percent change in total ozone column leads to about a -1.1% change in erythemally effective radiation [*Madronich et al.*, 1991]. Owing to the low variability of the ozone column observed during the campaign of ±2.3% (± 1 σ), the correction factors are small and range between 0.98 and 1.07. Thus, in Figure 7, the ratio (:= R_{ery}) of the normalized, erythemally weighted irradiance for all days to the values of January 11 are plotted versus the ratio (:= R_{total}) of the respective pyranometer measurements for SZA between 30° and 60°. The scatter in the plot is caused partly by the atmospheric conditions (e.g., cloud height and spatial

coverage) and partly by the sampling; the erythemally effective radiation was calculated from the spectral measurements, which take some minutes, whereas the total irradiance was measured only once per spectrum. Therefore rapid changes in cloud cover lead to a scatter in the correlation between erythemally effective radiation and pyranometer readings.

The correlation between change of the erythemally weighted irradiance and change of the total irradiance due to clouds has been quantitatively investigated for the atmospheric conditions prevailing in Lauder, New Zealand (45°S, 170°E) by *Bodeker and McKenzie* [1996]. For partly cloudy sky with the Sun obscured, they found that the attenuation of the erythemally weighted irradiance due to clouds is less than the reduction of the total irradiance. This is consistent with the observations in Townsville. Bodeker and McKenzie present similar scatterplots as shown in Figure 7. For $R_{\text{total}} < 1$, they parameterize these plots by a "cloud cover modifier (CCM) function":

$$\text{CCM} := A_{\text{SZA}} \cdot (R_{\text{total}})^{P_{\text{SZA}}} \quad (3)$$

The coefficients A_{SZA} and P_{SZA} of the fit function were found to be dependent on SZA. For SZA< 60°, A_{SZA} is approximately 1 and the power coefficient P_{SZA} varies between about 1.0 (0° SZA) and 0.8 (60° SZA). In order to compare the findings of Bodeker and McKenzie with the results obtained in this paper, the CCM functions for SZA = 30° and 60° are shown as well in Figure 7. More details on the interpretation of Figure 7 are given by *Bodeker and McKenzie* [1996].

5. Comparison With UV Measurements at Other Locations

The erythemally weighted irradiation calculated from the spectral measurements during Townsville campaign was compared with corresponding values given by *Seckmeyer et al.* [1995]. In this paper, geographical differences in the UV were quantified by comparing monthly means of the daily erythemal irradiation for summer months measured at 12 locations ranging from the South Pole to Barrow (71.2°N, 156.5°W), Alaska. Among these sites, Darwin (12.5°S, 130.8°E) is closest to the equator, and the cities Brisbane (27.5°S, 153.0°E), Perth (32.0°S, 115.8°E), and Melbourne (37.8°S, 144°E) are the three remaining Australian representatives of the survey. The study was based on data of spectroradiometers and broadband instruments which were calibrated against each other before the examination. Since the IFU mobile spectroradiometer took part herein, the results of the survey should compare well with the recent measurements in Townsville.

For the year 1991, the December and January values of the monthly mean daily erythemal irradiation found in the survey for Darwin, Brisbane and Perth are as follows: Darwin, 5.70 kJ/m^2 (December) and 3.72 kJ/m^2 (January); Brisbane, 4.76 kJ/m^2 (December) and 4.47 kJ/m^2 (January); Perth, 5.30 kJ/m^2 (December) and 5.77kJ/m^2 (January). The January value of Perth is also the highest value found in the study for all 12 locations and months. However, the average erythemal irradiation for the period of the recent campaign in Townsville is 6.06 kJ/m^2 and thus exceeds the January value of Perth by 5%. The pronounced difference of the December and January values for Darwin again shows the influence of cloud cover.

The importance of UV radiation for people living in Australia is demonstrated by the comparison of values of erythemally weighted irradiance measured in Townsville and during several years of measurement in Garmisch-Partenkirchen (47.5°N, 11°E, 730 m asl). The radiation levels observed in Townsville are clearly enhanced compared with the conditions in Germany. The erythemally weighted irradiance measured on midday of January 11 was 372 mW/m^2, and the highest value observed during the campaign was 429 mW/m^2. The highest value observed in clear skies Garmisch-Partenkirchen was 234 mW/m^2, and for all days, the highest value was 278 mW/m^2 [*Seckmeyer et al.*, 1994]. Thus maximum values for Townsville appear to be about 60% higher than the maxima observed in Garmisch-Partenkirchen.

The same applies for average values; as mentioned above, the average of the daily erythemally weighted irradiation for the period of the campaign was 6.06 kJ/m^2. For the period June 24 – July 21, the average values for Garmisch-Partenkirchen were 3.46 kJ/m^2 in 1994 and 3.70 kJ/m^2 in 1995. Hence the value for Townsville is increased by a factor of 1.75 (1994) and 1.64 (1995), respectively.

6. Discussion

A 1 month campaign is quite short, considering the large temporal (year to year) and spatial variability of UV radiation. Therefore it is not possible to set up a climatology of UV radiation within a short campaign. From the present knowledge [e.g., *McKenzie et al.*, 1994], the variability of global spectral UV irradiance on Earth depends mainly on variations of the solar elevation, cloud cover, total ozone column, aerosols, and albedo. In the following, it will be analyzed whether the parameters which influence the UV radiation were typical for the campaign. The examination will concentrate on the months December/January and on tropical Australia and will be based on pyranometer data, measurements of the total ozone column, and model calculations.

6.1. Temporal Variation

The temporal variation of UV irradiance during 1 day or between consecutive days was shown in Figures 2, 5, and 6. For the following investigation of the year-to-year variability, we assume that the variation mainly depends on differences in clouds and ozone.

6.1.1. Cloud cover. In Townsville, the summer may be sunny or rainy and therefore there is a pronounced year-to-year variability in cloudiness. This variability was quantified using pyranometric measurements which were carried out by the Bureau of Meteorology (BOM) at Townsville Airport, about 8 km from JCU. Data of the monthly averaged irradiation from the years 1971 to 1992 for the months December and January are examined. The minimum monthly mean during these 21 years occurred in December 1987 (8.95 MJ/m^2), and the maximum was measured in December 1972 (28.18 MJ/m^2). From these data, the long-term average and standard deviation for the period December 24 to January 20 can be estimated to be 22.00 ± 4.09 MJ/m^2. Thus the variation is ±18% of the mean at the ± 1 σ level.

From the pyranometric measurements carried out between December 24, 1995, and January 20, 1996, at JCU, the irradiation for each day was calculated. The mean of the daily irradiation is 21.76 MJ/m^2. Thus the daily mean irradiation is quite comparable with the long-term mean (22.00 MJ/m^2) measured by BOM. Therefore the assumption that the attenuation due to clouds showing typical values seems to be justified.

On the clear-sky day, January 11, the daily irradiation at JCU was 30.73 MJ/m^2. The ratio of the daily mean irradiation during the campaign to the irradiation of January 11 is 0.71, and the respective ratio of the erythemally effective doses is 0.78 (see Figure 6).

6.1.2. Ozone column. In Brisbane (1100 km from Townsville in the SSE direction), the total ozone column is monitored with a Dobson spectrometer which is also operated by BOM. Brisbane is the ozone-monitoring station closest to Townsville. From the Dobson measurement between 1989 and 1994, the mean total ozone column for the period December 24 to January 20 can be estimated to be 273 ± 4 DU (± 1 σ).

The average of the Dobson measurements for the days of the campaign was 268 DU and therefore quite comparable with the long-term mean of 273 DU. Generally, the variation of the ozone column is less pronounced at lower latitutes [*Larko and McPeters*, 1992]. Therefore it can be assumed that during the campaign, the ozone column for Townsville was within the long-term mean. Owing to the uncertainty of TOVS data (see above), these measurements, although available for Townsville, were not used for the analysis.

6.2. Spatial Variation

In order to answer the question of whether the conditions during the Townsville campaign were typical compared with other sites in tropical Australia, differences in solar elevation, altitude above sea level, and albedo between different locations must be considered in addition to the effects introduced by clouds and ozone. This will be done in the following.

According to our model calculations for clear sky, the erythemally weighted daily irradiation on January 1 at 19°S (Townsville) is 2.5% less than on the southern Tropic of Capricorn. At 10°S (northern border of Australia), it is 11% less, and at the equator, 25%. For these calculations, it was only considered that the course of the Sun on the sky during a day changes with latitude; all other factors were chosen equal (total ozone column, 260 DU; visibility, 200 km). For Townsville, the change in solar elevation during the campaign contributes less than 1% to the variability of the erythemally weighted irradiation.

A second important parameter is the difference in cloudiness observed at different locations; the closer to the equator the location, the more tropical the weather pattern, and the greater the influence of the summer wet season on the ambient solar UV radiation [*Roy et al.*, 1995]. Additionally, cloudiness depends on local conditions. The differences in cloud cover are therefore difficult to assess and were not investigated further in this study.

In order to address the spatial variability of the total ozone column, TOMS data recorded between 1989 and 1991 were analyzed [*Larko and McPeters*, 1992]. The data were averaged over longitude (-180° and +180°) and day (December 24 to January 20) for latitude bands of 10°. For the latitude band centered at 5° S, the mean total ozone column is 261 DU; for 15° S and 25°S, the respective values are 271 and 280 DU. Hence the difference in ozone concentration between 25°S and 10°S is approximately 14 DU or 5%. Owing to the decrease of the ozone column with decreasing latitude, UV levels at lower latitudes can be expected to be higher, but the absolute effect on erythemally weighted radiation should be small compared to the influence of solar elevation and cloudiness.

Most inhabitants of tropical Australia live near the coast and in regions below 200 m altitude. According to our model calculations, the increase of erythemally effective UV radiation within 200 m is below 2%. A part of the Australian tropics is covered with rain forests, and a part consists of desert. The albedo of sand is about 10% in the UV [*Blumthaler and Ambach*, 1988]. According to model calculations, UV levels for desert areas should be approximately 3% higher than for forested land.

7. Conclusions

The results of the 4 week campaign in Townsville presented in this study have shown high levels of UV radiation compared with midlatitudes. These levels are mainly caused by the high solar elevations and the relatively low stratospheric ozone concentrations in the tropics. However, from this short campaign it is not possible to set up a climatology of UV radiation. On the other hand, a more precise knowledge of the radiation environment is urgently needed because of the great impact of UV radiation on the biosphere including man. High incidence rates of skin cancer observed in the tropics which can be correlated to exposure to UV radiation clearly demonstrate the need for further research.

The comparison of measured and modeled global

spectral UV irradiance has confirmed that for clear-sky conditions, UV levels on Earth can be calculated fairly well. However, our ability to model the effects of clouds is still poor. Therefore a UV monitoring based on well-characterized spectroradiometers would be needed in order to set up a UV climatology and to detect possible changes in UV, regardless of whether these are caused by stratospheric ozone depletion or changes in cloudiness and aerosol loading of the atmosphere. Although, up until now, no significant trend in tropical UV radiation was reported, a suitable instrumentation should be established in the foreseeable future because a global climate change could also affect the tropics.

Acknowledgments. This work was funded by the German Ministry of Science, Education, Research and Technology. Special thanks are extended to the International Bureau of the DLR for supporting the collaboration between Germany and Australia. We thank the Australian Bureau of Meteorology for providing data of total irradiance and Dobson ozone measurements. Additionally, we thank A. Albold, M.J. Hulme, and V. Mohnen for their valuable comments to the manuscript.

References

Anderson, G. P., S. A. Clough, F. X. Kneizys, J. H. Chetwynd, and E. P. Shettle, AFGL Atmospheric Constituent Profiles (0-120 km), *AFGL Tech. Rep., AFGL-TR-86-0110*, Air Force Geophysical Laboratory, Air Force Base, Massachusetts, 1986.

Barton, I. J., The Australian UV-B monitoring network, *Tech. Pap. 46*, pp. 1-12, Aust. Div. of Atmos. Phys., Commonw. Sci. and Ind. Res. Organ., Melbourne, Victoria, 1983.

Blumthaler, M., and W. Ambach, Solar UVB-albedo of various surfaces, *Photochem. Photobiol., 48*(1), 85-88, 1988.

Bodeker, G. E., and R. L. McKenzie, An algorithm for inferring surface UV irradiance including cloud effects, *J. Appl. Meteorol., 35*(10), 1860-1877, 1996.

Bodhaine, B. A., R. L. McKenzie, P. V. Johnston, D. J. Hofmann, E. G. Dutton, R. C. Schnell, J. E. Barnes, S. C. Ryan, and M. Kotkamp, New ultraviolet spectroradiometer measurements at Mauna Loa observatory, *Geophys. Res. Lett., 23*(16), 2121-2124, 1996.

Bojkov, R. D., The changing ozone layer, *Publ. World Meteorol. Organ., Geneva, ISBN 92-63-10828-5*, 1995.

Bordewijk, J. A., H. Slaper, H. A. J. M. Reinen, and E. Schlamann, Total solar radiation and the influence of cloud and aerosols on the biologically effective UV, *Geophys. Res. Lett., 22*(16), 2151-2154, 1995.

Caldwell, M. M., and S. D. Flint, Stratospheric ozone reductions, solar UV-B radiation and terrestrial Ecosystems, *Clim. Change*, 28, 375–394, 1994.

German Institute of Standardization, Strahlungsphysik im optischen Bereich und Lichttechnik: Größen, Formelzeichen und Einheiten der Lichttechnik, *DIN 5031, part 3*, Beuth Verlag, Berlin, 1982.

Gies, H. P., C. R. Roy, S. Toomey, and D. Tomlinson, The ARL solar UVR measurement network: Calibration and results, in *Ultraviolet Technology V, Proc. SPIE Int. Soc. Opt. Eng., 2282*, 274-284, 1994.

Green, A., and D. Battistutta, Incidence and determinants of skin cancer in a high risk Australian population, *Int. J. Cancer, 46*, 356-361, 1990.

Harris, N. R. P., et al., Ozone measurements, in *Scientific Assessment of Ozone Depletion: 1994*, chap. 1, pp. 1.1-1.54, U. N. Environ. Programme, Nairobi, Kenya, 1994.

International Commission on Non-Ionizing Radiation Protection (ICNIRP) (Eds.), Global solar UV index, *ICNIRP 1/1995*, Bundesamt für Strahlenschutz, Oberschleissheim, Germany, 1995.

Jäger, H., G. Seckmeyer, B. Mayer, and R. Sladkovic, Observations at Garmisch-Partenkirchen related to a vortex passage in January 1995, in *Polar Stratospheric Ozone, Proceedings of the Third European Workshop 18 to 22 September 1995, Schliersee, Bavaria, Germany, Air Pollut. Res. Rep. 56,* edited by J. A. Pyle, N. R. P. Harris, and G. T. Amanatidis, Offi. for Off. Publ. of the Eur. Communities, Luxembourg, 1996.

Larko, D., and R. McPeters (Eds.), TOMS ozone data 1989-1991, CD-ROM, USA_NASA_UARP_OPT_003, version 6.0, NASA Goddard Space Flight Center, Greenbelt, Md., 1992.

Madronich, S., L. O. Björn, M. Ilyas, and M. M. Caldwell, Changes in biologically active ultraviolet radiation reaching the earth's surface, in *Environmental Effects of Ozone Depletion: 1991 Update*, pp. 1-13, U. N. Environ. Programme, Nairobi, Kenya, 1991.

Marks, R., M. Staples, and G. G. Giles, Trends in non-melanocytic skin cancer treated in Australia: The second national survey, *Int. J. Cancer 53*, 585-590, 1993.

McKenzie, R. L., M. Kotkamp, G. Seckmeyer, R. Erb, C. R. Roy, H. P. Gies, and S. J. Toomey, First southern hemisphere intercomparison of solar UV spectra, *Geophys. Res. Lett., 20*(20), 2223-2226, 1993.

McKenzie, R. L., M. Blumthaler, C. R. Booth, S. B. Diaz, J. E. Frederick, T. Ito, S. Madronich, and G. Seckmeyer, Surface ultraviolet radiation, in *Scientific Assessment of Ozone Depletion: 1994*, chap. 9, pp. 9.1-9.22, U. N. Environ. Programme, Nairobi, Kenya, 1994.

McKinlay, A. F., and B. L. Diffey, A reference action spectrum for ultraviolet induced erythema in human skin, Commission Internationale de l'Éclairage, 6(1), 17-22, 1987.

Molina, L. T., and M. J. Molina, Absolute absorption cross section of ozone in the 185 to 350 nm wavelength range, *J. Geophys. Res., 91*(D13), 14,501-14,508, 1986.

Nack, M. L., and A. E. S. Green, Influence of clouds, haze, and smog on the middle ultraviolet reaching the ground, *Appl. Opt., 13*(10), 2405-2415, 1974.

Robertson, D. F., Solar ultraviolet radiation in relation to human sunburn and skin cancer, Ph.D. thesis, Department of Physics, University of Queensland, Brisbane, Australia, 1972.

Roy, C. R., H. P. Gies, and S. Toomey, The solar UV radiation environment: Measurement techniques and results, *J. Photochem. Photobiol. B: Biology, 31*, 21-27, 1995.

Schaart, F.-M., C. Garbe, and C. E. Orfanos, Ozonabnahme und Hautkrebs: Versuch einer Risikoabschätzung, *Der Hautarzt, 44*, 63-68, 1993.

Seckmeyer, G., and G. Bernhard, Cosine error correction of spectral UV irradiances, in *Atmopheric Radiation, Proc. SPIE Int. Soc. Opt. Eng.*, 2049, 140-151, 1993.

Seckmeyer, G., and R. L. McKenzie, Increased ultraviolet radiation in New Zealand (45°S) relative to Germany (48°N), *Nature, 359*, 135-137, 1992.

Seckmeyer, G., B. Mayer, R. Erb, and G. Bernhard, UVB in Germany higher in 1993 than in 1992, *Geophys. Res. Lett., 21*(7), 577-580, 1994.

Seckmeyer, G., et al., Geographical differences in the UV measured by intercompared spectroradiometers, *Geophys. Res. Lett., 22*(14), 1889-1892, 1995.

Seckmeyer, G., G. Bernhard, B. Mayer, and R. Erb, High

accuracy spectroradiometry of solar ultraviolet radiation, *Metrologia, 32*(6), 697-700, 1996.

Setlow, R. B., The wavelengths in sunlight effective in producing skin cancer: A theoretical analysis, *Proc. Nat. Acad. Sci. U.S.A, 71*(9), 3363-3366, 1974.

Stamnes, K., S. C. Tsay, W. Wiscombe, and K. Jayaweera, A numerically stable algorithm for discrete-ordinate-method radiative transfer in multiple scattering and emitting layered media, *Appl. Opt., 27*(12), 2502 - 2509, 1988.

Stamnes K., J. Slusser, and M. Bowen, Derivation of total ozone abundance and cloud effect from spectral irradiance measurements, *Applied Optics, 30*(30), 4418-4426, 1991.

Woods, T. N., et al., Validation of the UARS solar ultraviolet irradiances: Comparison with the ATLAS 1 and 2 measurements, *J. Geophys. Res., 101*(D6), 9541-9569, 1996.

World Health Organization (Eds.), *Environmental Health Criteria 160, Ultraviolet Radiation*, WHO and Int. Comm. on Non-Ionizing Radiat. Prot., Geneva, 1994.

G. Bernhard, B. Mayer, and G. Seckmeyer, Fraunhofer Institute for Atmospheric Environmental Research, Kreuzeckbahnstr. 19, D-82467 Garmisch-Partenkirchen, Germany. (e-mail: uvb@ifu.fhg.de)

A. Moise, Department of Physics, James Cook University of North Queensland, Townsville 4811, Queensland, Australia. (e-mail: aurel.moise@jcu.edu.au)

(Received August 29, 1996; revised December 26, 1996; accepted December 26, 1996.)